

# Detection of vegetation changes in high resolution satellite imageries with Support Vector Machines and Mahalanobis distance algorithms

Fernando, Rodríguez Berrocal<sup>1</sup>, José. A. Malpica Velasco<sup>2</sup>

<sup>1</sup>Mathematics Department, Faculty of Science, University of Alcalá,  
Campus Universitario. Ctra. Madrid-Barcelona, Km. 33,600,28871 Madrid, Spain  
vanarles@hotmail.com

<sup>2</sup>Mathematics Department, Faculty of Science, University of Alcalá,  
Campus Universitario. Ctra. Madrid-Barcelona, Km. 33,600,28871 Madrid, Spain  
josea.malpica@uah.com

**Abstract.** Our objective is to compare the effectiveness of two algorithms, the Support Vector Machine (SVM) and the Mahalanobis distance, for the detection of vegetation changes in multispectral satellite images taken on two different dates. Classification methods are applied to each image to obtain a layer of probability of the vegetation, and later to detect possible changes. For this study two high-resolution satellite images taken in the 2005 and 2006 summers were used. Training the classification with very few pixels, Mahalanobis and SVM proved to be almost similar, however the latter algorithm shows a slight advantage in the visualization of changes.

**Keywords:** Mahalanobis distance, SVM, ROC curves, SPOT 5 satellite.

## 1 Introduction

Increased public awareness and concern about environmental issues have increased the demand on data related to vegetation. In this sense, the qualitative and quantitative assessment of changes in vegetation is an important issue in ecological studies and in different branches of Earth science. Today most of these temporary studies are performed through visual analysis of images by experts. Due to the large number of these images, automatic methods are needed as basic aids for these analyses in their daily work.

Modern technologies, such as Geographic Information Systems (GIS) and Remote Sensing, have facilitated the investigation of complex spatial patterns, which have a time variation as with vegetation. The success of automated methods for detecting changes is based on a good classification of satellite images. This task is very costly in time and resources, especially with regard to field visits in order to establish training areas.

## 2 Materials and Methods

### 2.1 Data Set

For our study we used high-spatial resolution images from the SPOT 5 satellite. This was launched on the May 2, 2002, and was the fifth in the SPOT series. The main innovation introduced by the SPOT 5 is the high resolution stereoscopic instrument. By complex processing techniques, SPOT 5 is capable of generating images of 2.5 m spatial resolution from two images of 5 m. The resolution (see Table 1) for bands B1, B2, and B3 is 10 m, while for B4 it is 20 m.

**Table 1.** SPOT 5 characteristics

Features	SPOT 5
Spectral bands	P: 0.49-0.69 (Panchromatic, 2.5 m) B1: 0.50-0.59 (Green, 10 m) B2: 0.61-0.68 (Red, 10 m) B3: 0.79-0.89 (Near-infrared, 10 m) B4: 1.58-1.78 (Middle-infrared, 20 m)
Sensor footprint	60 km x 60 km
Revisit interval	Every 26 days

SPOT 5 provides a good balance between high resolution and the image capture field, which is 60 km x 60 km. The images were taken in an area near Madrid, Spain. The first image was taken on July 24, 2005, at 11:09 GMT, with an incidence angle of  $3.12^\circ$  and an azimuth of  $14.01^\circ$ . The sun had an elevation angle of  $44.23^\circ$  and an azimuth of  $166.69^\circ$  (Figure 1a). The second image is from August 6, 2006, at 11:23 GMT. The incidence angle is  $20.05^\circ$  and the azimuth is  $16.38^\circ$ , while the sun's elevation angle is  $62.37^\circ$  and its azimuth is  $150.06^\circ$  (Figure 1b).

**Fig. 1.** Color composites of SPOT 5, with 1, 2, and 3 bands for RGB, 2005 (a) and 2006 (b).

## 2.2 Preprocessing

The images were georeferenced to the European datum using the ephemerides of the satellite and three ground control points. Precisions better than one pixel were obtained. The co-registration was not necessary. Earth observation satellites provide us with multispectral and panchromatic data with different resolutions, spatial and spectral, temporal and radiometric. To detect changes and determine classification accuracy, is necessary to define a single image containing information of multispectral and panchromatic bands. This technique, known as pan-sharpening, tries to preserve the multispectral information while trying to increase the spatial resolution as much as possible. In our case, the pan-sharpening algorithm principal component analysis was applied to both images, obtaining a resolution of 2.5 m.

Another important point discussed in this section is the radiometric correction and standardization due to atmospheric conditions. In our case it is not necessary to make this correction because the proposed method calculates a probability layer independently for each image. As Singh [2] stated, when images are classified independently, the effects due to different atmospheric conditions and different sensors for multispectral image acquisition can be minimized. Therefore, no radiometric correction were used.

## 2.3 Classification Algorithms

The algorithms used for the classification were the Support Vector Machine (SVM) and the Mahalanobis distance. Below, both algorithms are briefly explained. Refer to [4] for more details about the SVM and to [1] for Mahalanobis distance.

### 2.3.1 The Mahalanobis Distance

To find out to which class each pixel belongs, the following probabilities must be calculated:

$$P(\omega_i | \vec{x}), i = 1, 2,$$

Where  $\omega_i$  are the classes ( $i=1, 2$ ) and  $\vec{x}$  is the vector of the pixel samples, A pixel is assigned to the object of interest if its conditional probability is the largest:

$$x \in \omega_i \Leftrightarrow P(\omega_i | \vec{x}) \geq P(\omega_j | \vec{x}) \quad \forall j \neq i$$

Here we assume that there is a set of training pixels. Assuming a Gaussian distribution for each class and after some mathematical operations, the formula of the Mahalanobis distance  $\delta$  is obtained as:

$$\delta = \sqrt{(\vec{x} - \vec{m})^T \Sigma^{-1} (\vec{x} - \vec{m})}$$

where

$\vec{m}$  is the mean vector of the pixels for the class under analysis,  
 $\Sigma$  is the variance-covariance matrix of pixel values of the class.

After calculating the Mahalanobis distance for each pixel of the image, we normalize the distances to a range of values [0,1] to be compared with the results produced by the SVM. Thus, a pixel with a Mahalanobis distance of 0 will be assigned a probability of 1. The greater the distance, the lower the probability, and vice versa.

### 2.3.2 Support Vector Machine

The SVM algorithm is formed by a group of supervised learning methods that can be applied to classification and regression. From a theoretical point of view, it is based on statistical learning theory proposed by Vapnik and Chervonenkis in the 1960s.

Given two sets (classes) of different data, the goal of SVM is to determine which of the two classes belong to a new data point. Each data will be interpreted, in SVM, as a vector of  $n$  dimensions, and the algorithm will try to separate these two classes by generating a hyperplane. Many hyperplanes can separate the two classes, but only one will be chosen maximizing the distance to the nearest points of each class.

## 2.4 Training

Due to the displacement toward the infrared region of the SPOT 5 sensor, green vegetation is shown in the red color, as can be seen in Figure 2a. This is convenient for differentiating green vegetation from the other objects and facilitates the choice of training areas for classification. These can be seen in detail in Figure 2b for the SPOT 5 image of 2006.



**Fig.2.** Training samples and details

### 3 Results and Discussion

The figures presented below show the results for each classifier on the two studied dates.

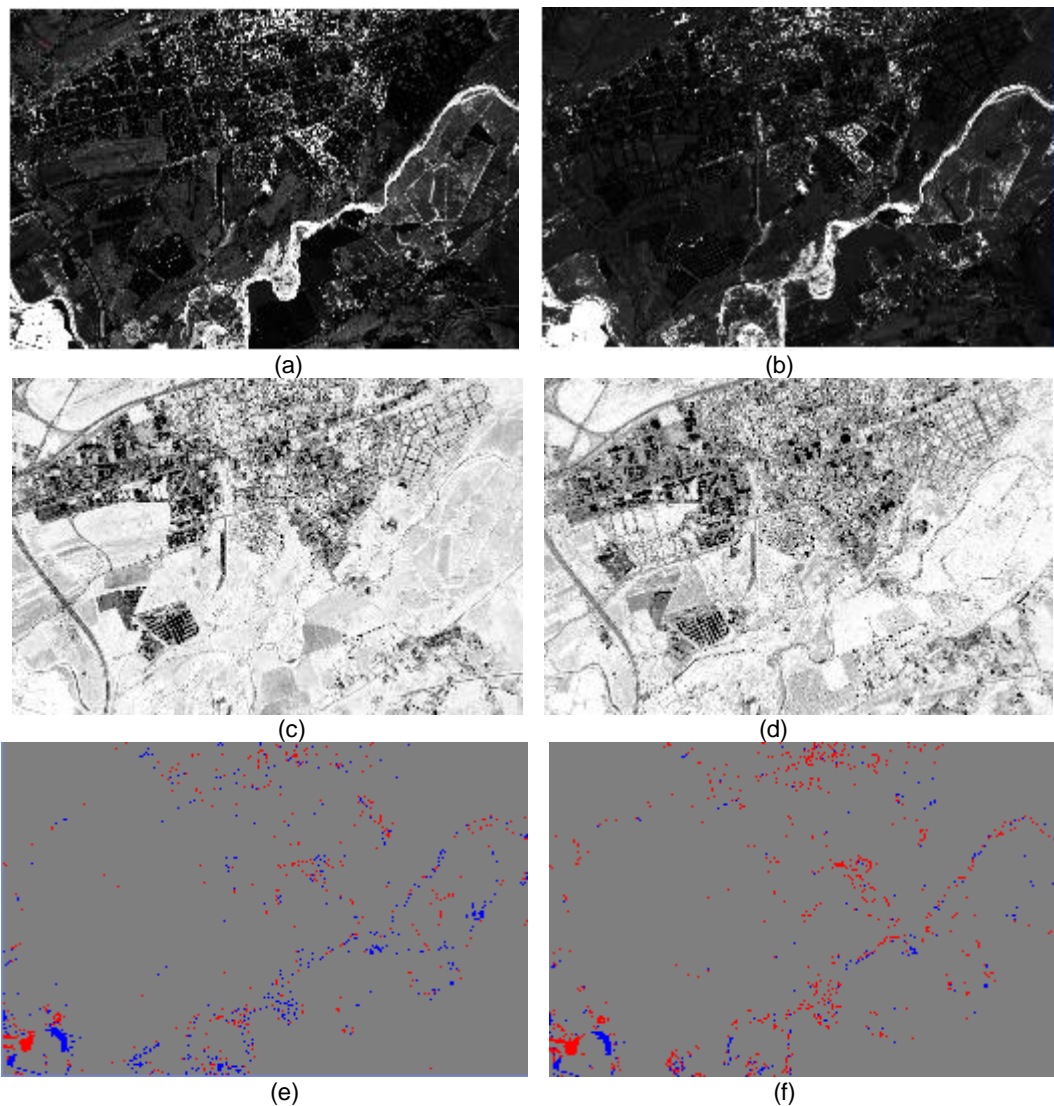


**Fig.3.** Different result images: SVM for 2005 (a) and 2006 (b); Mahalanobis for 2005 (c) and 2006 (d); difference for SVM (e) and difference for Mahalanobis (f).

In the case of Mahalanobis, the probability layers are not obtained directly as with SVM. Data (distances) must be transformed to probabilities. In SVM, the longer the distance of the pixel to the flat hyperplane, the higher the probability that it belongs to the class of interest. The same is true when applying the Mahalanobis distance. For the Mahalanobis distance, the smaller the Mahalanobis distance, the higher the probability. For the case of the Mahalanobis, as shown in Figure 3c and 3d, distinguishing green vegetation from any other element in the study area is very difficult. If we want a greater contrast between classes, it is necessary to increase the number of pixels (initially only 100 pixels were chosen) for the training area of vegetation; this will also improve the detection of changes. Figure 3e and 3f shows the difference in probability layers created from the Mahalanobis and SVM on bitemporal images of the SPOT 5. The result of these changes is regulated by two colors, the blue pixels represent "positive" changes in vegetation, i.e., where there was vegetation in 2006 that was not there in 2005, and the red pixels represent "negative" changes, i.e., where there was vegetation in 2005 that was not there in 2006.

To examine the layers of differences, we look at two cuts of the image under study for each of the classifiers. Figure 4 refers to such cuts. In the image for 2005, a gray-blue elongated strip with no vegetation can be seen; however, this is shown as vegetation in 2006. Figure 4c shows that the SVM defines the area of vegetation in a more precise way than the Mahalanobis (Figure 4d). Moreover, the SVM shows very small changes that the Mahalanobis distance does not. This is because the SVM uses a hyperplane to separate the pixels belonging to green vegetation from those that do not belong to it, while the Mahalanobis distance uses in its definition the covariance matrix, spreading the discriminate information of the classifier.

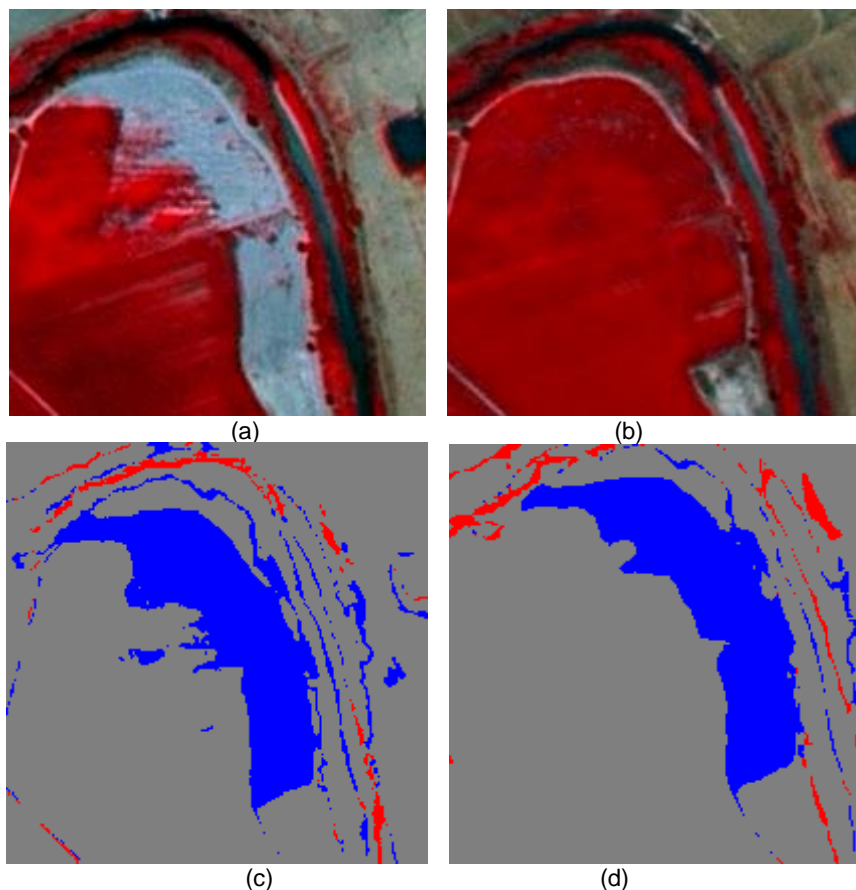


**Fig.4.** Image detail studied in 2005 (a) and 2006 (b); difference for the SVM (c) and difference for the Mahalanobis (d).

To complete the visual analysis and to determine if a classification is better or worse, we carried out a numerical evaluation. The method chosen was the Receiver Operating Characteristic (ROC) curves because confusion matrices are not effective due to the high classification accuracy of vegetation for both methods in this type of imagery. In these, abscises represent the probability of false alarm and ordinates the probability of detection. Refer to Swets [3] for more details about the ROC curves.

It would be interesting to compare these classification methods with the differences between NIR bands, this comparison remains to be done in the future.

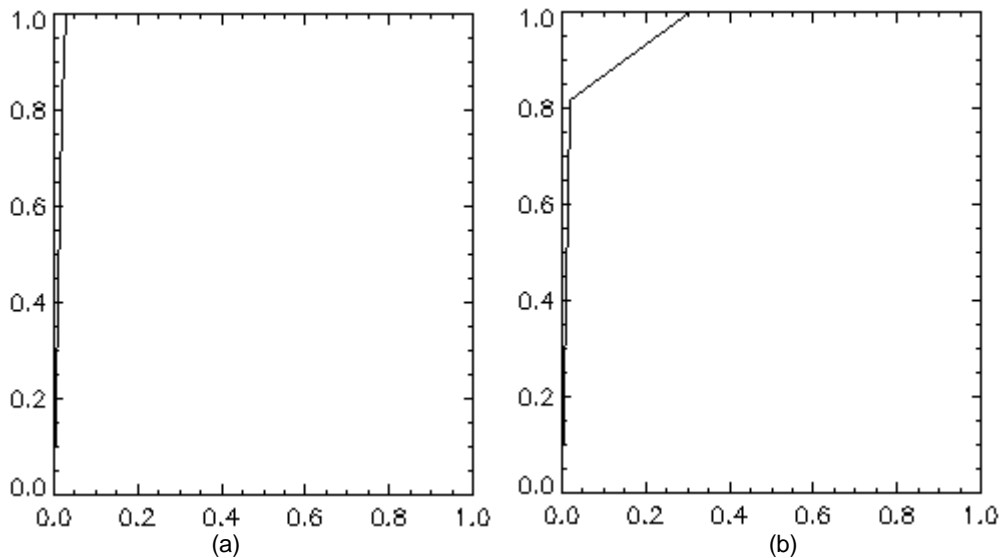


**Fig.5.** The ROC curves.

The accuracy of the classifier can be measured by the area under the ROC curve. An area of 1 represents a perfect test and an area of 0.5 represents a worthless test. Between these limits we have the following categories: 0.5-0.6, fail; 0.6-0.7, poor; 0.7-0.8, fair; 0.8-0.9, good; and 0.9-1, excellent. The area under the curve for our experiment gives: 0.99312 for the SVM and 0.93485 for the Mahalanobis distance. Both are excellent. Hence, it cannot be said that one algorithm is better than the other. The shape of the ROC curve offers interesting conclusions on this aspect. If we look at Figure 5a and 5b, we see that the SVM is more effective than the Mahalanobis in detecting false alarms in the high values of probability of detection.

## 4 Conclusions

The algorithms proposed in this study have proven useful in detecting vegetation changes in high-resolution satellite images without field visits and with a minimum number of pixels for training the classification. The result shows that the SVM and Mahalanobis distance are similar with respect to the area of the ROC curves, both with a value of more than 0.9. However, visually we found that the changes were shown more precisely by the SVM than the Mahalanobis distance. Moreover, areas with a very small change are shown only with the SVM classifier.

## Acknowledgments

The authors wish to thank the Spanish National Mapping Agency (Instituto Geográfico Nacional) for providing the images for this study, and to the Spanish Ministry of Science and Innovation (project CGL2009-13768) for financial support for presenting this paper.

## References

- [1] Richards, John A., Xiuping Jia, 2006. *Remote Sensing Digital Image Analysis: An Introduction*, 4th edn., 439 páginas. Springer, Heidelberg.
- [2] Singh, A., 1989. Digital change detection techniques using remotely sensed data, *International Journal of Remote Sensing* 10 (6), 989-1003.
- [3] Swets, J.A., 1979. *ROC analysis applied to the evaluation of medical imaging techniques*,

*Investigate Radiology*, 14: 109-121.

[4] Vapnik, V., 1995 *The Nature of Statistical Learning Theory*. Springer, New York.